

## Cooperative Dynamics in Two Dimensions

Ronen Zangi

*Department of Biophysical Chemistry, University of Groningen, Nijenborgh 4, 9747 AG Groningen, The Netherlands*

Stuart A. Rice

*Department of Chemistry and The James Franck Institute, The University of Chicago, Chicago, Illinois 60637, USA*

(Received 12 June 2003; published 22 January 2004)

We report results from molecular dynamics simulations of cooperative motion in a quasi-two-dimensional system of colloid particles. We find that the onset of the deviation of the single-particle displacement distribution from Gaussian form starts in the liquid phase and extends, with increasing magnitude, through the hexatic phase into the crystalline phase. The time for which the deviation is maximum increases exponentially with the density. As the density increases toward the hexatic phase a third dynamical relaxation mode emerges. We argue that the collective motion is generated by superpositions of instantaneous normal mode vibrations, with lifetimes that increase with the density, along paths with strong bond-orientation correlation.

DOI: 10.1103/PhysRevLett.92.035502

PACS numbers: 61.20.Ja, 61.20.Lc, 66.30.-h, 82.70.Dd

The Gaussian form of the single-particle displacement distribution is obtained, rigorously, for two limiting cases. The first case is for  $t \rightarrow 0$ , representing ballistic motion, leading to a mean squared displacement that is a quadratic function of time. The second case is for  $t \rightarrow \infty$ , describing Brownian motion (hydrodynamic regime), leading to a mean squared displacement that is a linear function of time. In both of these time regimes the particle displacement vector orientations are randomly distributed. Deviations from a Gaussian distribution signal correlations between the displacement vectors of the particles. In three dimensions the interpolation between the short and long time dynamics extends over a short time period and the deviations from Gaussian behavior are very small [1,2]. However, strong deviations have been observed in dense glass-forming liquids just above the glass transition [3–8].

Recently, it has been shown, both computationally [9–12] and experimentally [13,14], that the motion of a particle in a dense quasi-two-dimensional (Q2D) liquid is heterogeneous and the single-particle displacement distribution has a very large non-Gaussian component. Moreover, it is found that in a Q2D liquid the single-particle displacement involves cooperative stringlike motion in some time regimes. Marcus, Schofield, and Rice found that in a dense Q2D colloid suspension the self-part of the van Hove function develops a second peak due to an activated process in which a particle hops to one of the positions that was formerly occupied by one of the cage particles that initially surrounded it [13]. Cui, Lin, and Rice [14] found that the one-particle displacement dynamics can be described in terms of three relaxation processes; the contributions of these processes to the particle mean squared displacement vary with time so that one or the other is dominant in different time domains. In this Letter we investigate the density depen-

dence of the deviation of the single-particle displacement distribution from Gaussian form as the system transforms from liquid through hexatic to the solid phase.

The model systems that we study consist of a single layer, with  $N = 2016$  particles, placed in a quasi-two-dimensional simulation box. The calculations were carried out, and the results are reported below, in terms of the reduced variables  $r^* = r/\sigma$ ,  $z^* = z/\sigma$ ,  $T^* = k_B T/\epsilon$ ,  $\rho^* = \rho\sigma^2$ ,  $t^* = t(k_B T/m\sigma^2)^{1/2}$ ,  $m = 1$ , with  $\sigma$  the diameter of the particle,  $\rho$  the number density,  $m$  the mass of the particle,  $t$  the time, and  $3.689\epsilon$  is the value of the interparticle potential at  $r^* = 1.000$ . We characterize the state of the system with the two-dimensional number density  $\rho = N/A$ , where  $A$  is the area of the simulation cell in the  $x$ - $y$  plane. The interparticle potential was represented by  $u(r^*) = A(r^* - 1/2)^{-\alpha}$  with  $A = 2 \times 10^{-19}$  and  $\alpha = 64$ . This functional form is very nearly a hard-core repulsion but has continuous derivatives. The confinement of the particles along the  $z$  axis is affected by the action of a one-body  $z$ -dependent external field,  $u_{\text{ext}}(z^*) = D\epsilon(z^*)^\zeta$ . The coordinate  $z^*$  is the distance from the center of the cell to the center of mass of the particle,  $\zeta = 24$  and  $D = 2 \times 10^{24}$ ; this potential confines the particles as if they were in a cell with an effective height of  $H = 1.20\sigma$ . The molecular dynamics (MD) simulations were performed in the microcanonical ensemble using the “velocity Verlet” algorithm. The distance at which the potential was cut off was  $1.5\sigma$  and the time step used was, in reduced units,  $5 \times 10^{-4}$ ; the associated rms fluctuation in total energy did not exceed one part in  $10^5$ . Equilibration for at least  $1.2 \times 10^7$  MD steps preceded the time-dependent data collection stage. Additional description of the methods used can be found in a previous report that investigated the thermodynamic properties of colloidal particles interacting with similar but slightly different pair potentials [15].

Analysis of the lateral-pressure-density isotherm and the character of the structural (translational and bond-orientation) properties of the system indicate that for densities  $\rho^* \leq 0.860$  the system is in the liquid phase, for densities  $0.870 \leq \rho^* \leq 0.890$  it is in the hexatic phase and for densities  $\rho^* \geq 0.900$  it is in the solid phase. As a measure of the deviation of the single-particle displacement from Gaussian form we calculate the non-Gaussian parameter  $\alpha_2(t)$ . It is plotted in Fig. 1 as a function of the reduced time for  $0.860 \leq \rho^* \leq 0.920$ . The value of  $\alpha_2(t^*)$  exhibits a maximum whose magnitude increases as the density increases. The time for which  $\alpha_2(t^*)$  is maximum,  $t_{\max}^*$ , increases exponentially with the density. Despite the small amplitude of  $\alpha_2(t^*)$  for  $\rho^* \leq 0.860$ , analysis of the trajectories reveals correlated heterogeneous dynamics. However, as the density increases towards the density that supports the hexatic phase,  $\rho^* = 0.870$ , there is a sharp increase in the magnitude of  $\alpha_2(t^*)$  that extends into the solid phase. Note that the time for which the maximum of  $\alpha_2(t^*)$  is observed encompasses many collision events. For example, the maximum for  $\rho^* = 0.890$  occurs at around  $t_{\max}^* = 35$  corresponding to 180 collision times. For  $\rho^* = 0.910$  the maximum of  $\alpha_2(t^*)$  is observed at  $t_{\max}^* = 3000$  which corresponds to  $1.7 \times 10^4$  collision times.

In Fig. 2 we display the lateral mean squared single-particle displacement as a function of the reduced time on a logarithmic scale. For time shorter than the particle collision time ( $t^* \leq 0.1$ ) the plots for all densities overlap as expected for density independent ballistic motion (the slope is equal to 2). At long time the motion is diffusive (the slope is equal to 1) for all densities even for those that correspond to the solid phase. As the density approaches the transition to the hexatic phase from below a third dynamical relaxation mode, at intermediate time,

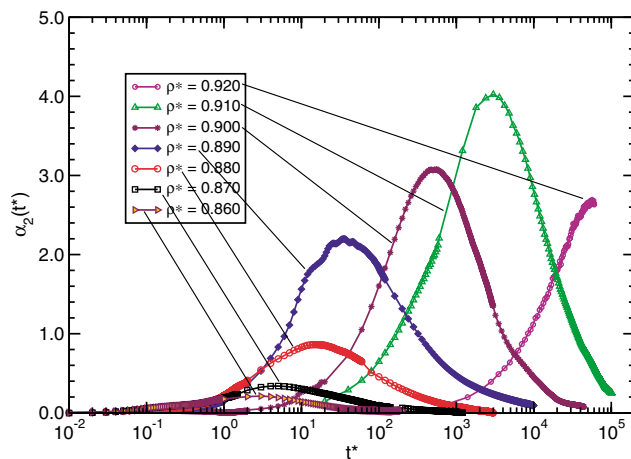


FIG. 1 (color online). The non-Gaussian parameter  $\alpha_2(t^*)$  as a function of the reduced time,  $t^*$ , for two-dimensional number densities  $0.860 \leq \rho^* \leq 0.920$ . The  $x$  axis is plotted on a logarithmic scale.

emerges. It represents a slowing down in the particle motion due to the “cage effect.” The slope for this intermediate dynamical relaxation mode is sublinear for densities lower, and vanishes for densities higher, than the melting density ( $\rho^* = 0.895$ ). This is a consequence of dynamical heterogeneity; the system consists of dynamically “ordered” and “disordered” domains. The motion of the particles in the disordered domain during  $t_{\max}$  is cooperative and quasi-one-dimensional (stringlike), yielding the observed deviation from the Gaussian form of the displacement distribution. The resulting displacement dynamics, therefore, has a mixed character. Note that the onset of the long time dynamical relaxation mode is the same as  $t_{\max}^*$  identified in Fig. 1.

Figure 3 shows the trajectory of the particles for a section of the simulation box for  $\rho^* = 0.880$ . The time covered is in the range  $0 \leq t^* \leq 100$ , which is about  $6t_{\max}^*$ . For this density and for this time interval the mean squared displacement,  $\langle \Delta r_{xy}^2(t^* = 100) \rangle = 3.78$ . Thus, the trajectories of most of the particles in this figure represent diffusion for a distance of about two particle diameters. The correlated and heterogeneous dynamics of the particles can be clearly identified as well as the diffusive paths which are along the directions with strong bond-orientation correlation.

The time-dependent distribution of the particle motion was analyzed using the van Hove functions. At short and long times we find that the self-part of the van Hove function is almost identical to the distribution derived from the Gaussian approximation. As shown above, there is a correlation between the location of  $t_{\max}$  and the time for which the diffusive behavior begins. We find that at the transition from intermediate time to long time the single-particle displacement distribution exhibits strong deviation from the Gaussian approximation. Figure 4(a) displays the self-part of the van Hove function for 4 times

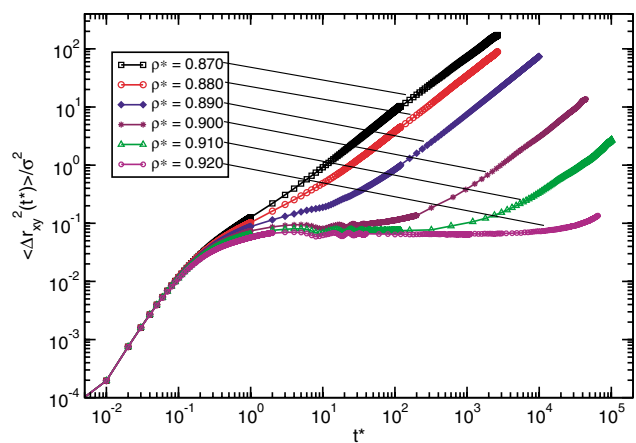


FIG. 2 (color online). The lateral mean squared displacement as a function of the reduced time,  $t^*$ , for two-dimensional number densities  $0.870 \leq \rho^* \leq 0.920$ . Both axes are plotted on a logarithmic scale.

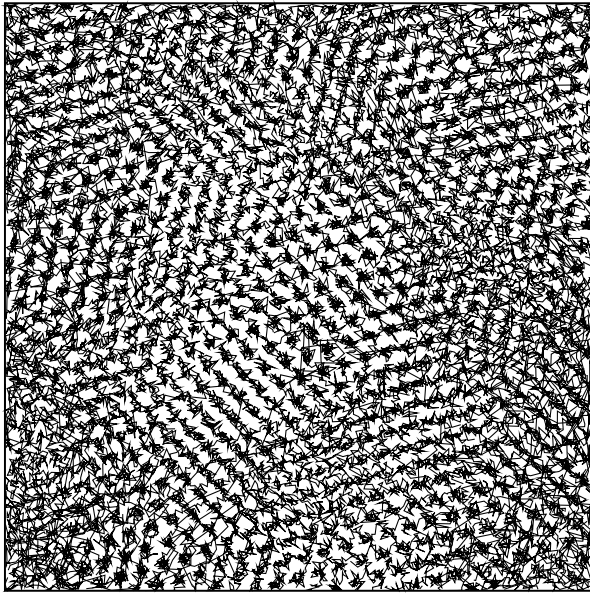


FIG. 3. A section of the simulation box for  $\rho^* = 0.880$  showing the particle trajectories. The total number of frames is 41 separated by time interval  $\Delta t^* = 2.5$ , so that the duration of each trajectory is  $t^* = 100$ . At this density,  $t_{\max}^* = 16$  and  $\langle \Delta r_{xy}^2(t^* = 100) \rangle = 3.78$ .

around  $t_{\max}^*$ . The curves exhibit multiple maxima indicating that the dynamics is heterogeneous and that the particles experience cooperative “jumps” from one site to another. Thus, at specific values of time there are different subsets of particles that travel for different distances. The fact that these maxima are separated by a distance that corresponds the particle diameter indicates that the jump dynamics, over 2–3 particle diameters, is in one dimension. Figure 4(b) displays the corresponding distinct part of the van Hove function. It is evident that as  $t^*$  increases the probability of finding a particle at the location where another particle resided at  $t^* = 0$  increases dramatically. The minimum of the probability distribution at  $r_{xy}^* = 0.5$  confirms the picture of jumps rather than continuous diffusion.

Correlated jump dynamics also occurs in the solid phase. Figure 5(a) displays the self-part of the van Hove function for  $\rho^* = 0.910$  at times in the range  $2500 \leq t^* \leq 140\,000$ . The curves are similar to those shown in Fig. 4(a). However, the number of maxima is larger and they are better resolved, which indicates greater heterogeneity and stronger dynamical correlations. Figure 5(b) displays the corresponding distinct part of the van Hove function; it shows a large increase at  $r_{xy} = 0.0$  as the time increases while for larger values of  $r_{xy}$  it is hardly changed. Figure 2 shows that at very long time the colloid particle motion for all densities, even for densities in the solid phase, is diffusive.

The results presented in this Letter reveal a strong correlation between the dynamical and the thermody-

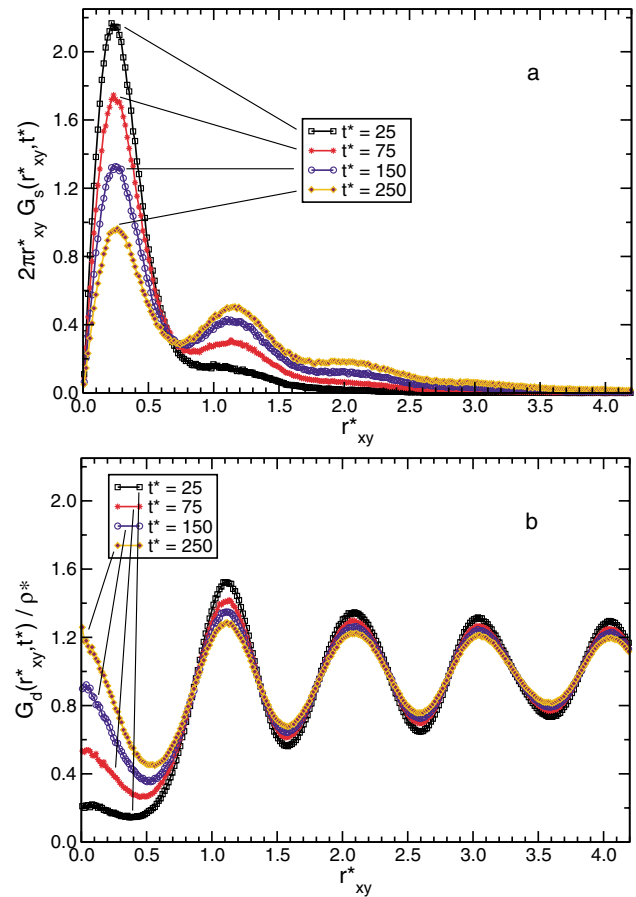


FIG. 4 (color online). The self-part (a) and the distinct-part (b) of the van Hove function as a function of the reduced lateral interparticle distance, plotted for  $\rho^* = 0.890$  at four values of time around  $t_{\max}^* \sim 35$ . The former is multiplied by the radial element  $2\pi r_{xy}$  and the latter is normalized by the reduced two-dimensional number density.

namic behavior of a quasi-two-dimensional system. Although dynamical heterogeneity and correlated motion are present in the liquid phase, at the liquidus the distribution of single-particle displacements develops a strong deviation from Gaussian form and the mean squared displacement as a function of time exhibits a third relaxation region, at intermediate times, that is characterized by a sublinear slope. The onset of this behavior is associated with the transition from the liquid to a hexatic phase with long-ranged bond-orientation order. At the solidus this sublinear slope becomes zero for intermediate time.

The continuous behavior of this mode of motion from the liquid phase through the hexatic phase and into the crystalline phase suggests that it arises from the same physical phenomenon. It is logical to assign the driver for motion in the solid phase to superpositions of normal mode vibrations along paths that generate activated hopping of a particle [16,17]. In the liquid phase the lifetimes of the normal modes vibrations are very short due to

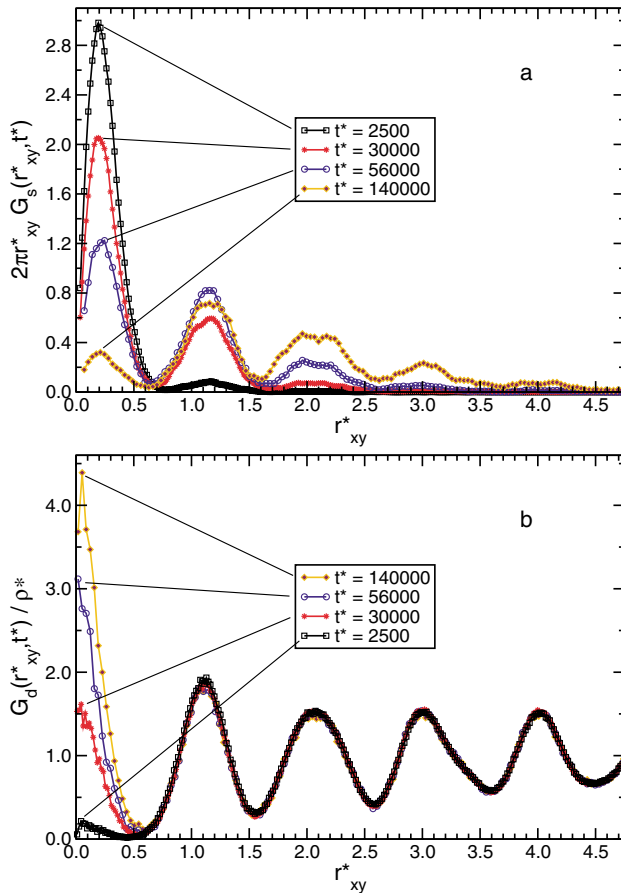


FIG. 5 (color online). Same as Fig. 4 but for a density that corresponds to the solid phase,  $\rho^* = 0.910$ .

preemption by independent single-particle motion [18], but instantaneous normal modes can be defined, and are found to be very useful descriptors [19,20]. Instantaneous normal modes are defined by expansion of the potential energy of the system about the positions of the particles in a frozen (instantaneous) configuration. Because not all particles are at potential minima, some of the instantaneous modes are imaginary. Nevertheless, they provide an interesting and often useful description of atomic dynamics in a liquid.

As the density increases (or the temperature decreases) the lifetimes of the instantaneous normal vibrations increase, thereby allowing more effective competition between cooperative hopping motion and independent

particle motion, so that the cooperative hopping becomes increasingly dominant [21]. We suggest that the correlated motion, even at densities lower than the solidus density, is a result of superposition of instantaneous normal mode excitations with energy greater than the energy barrier for hopping. The natural hopping directions are along axes with strong bond-orientation correlation that are developed at the transition to the hexatic phase.

This research was supported by EC Contract No. MCFI-1999-00161 and by the National Science Foundation via Grant No. NSF-CHE 9977841.

- [1] A. Rahman, Phys. Rev. **136**, A405 (1964).
- [2] D. Levesque and L. Verlet, Phys. Rev. A **2**, 2514 (1970).
- [3] A. Heuer and K. Okun, J. Chem. Phys. **106**, 6176 (1997).
- [4] W. Kob, C. Donati, S. J. Plimpton, P. H. Poole, and S. C. Glotzer, Phys. Rev. Lett. **79**, 2827 (1997).
- [5] C. Donati *et al.*, Phys. Rev. Lett. **80**, 2338 (1998).
- [6] W. K. Kegel and A. van Blaaderen, Science **287**, 290 (2000).
- [7] E. R. Weeks, J. C. Crocker, A. C. Levitt, A. Schofield, and D. A. Weitz, Science **287**, 627 (2000).
- [8] Y. Gebremichael, T. B. Schroder, F. W. Starr, and S. C. Glotzer, Phys. Rev. E **64**, 051503 (2001).
- [9] M. M. Hurley and P. Harrowell, Phys. Rev. E **52**, 1694 (1995).
- [10] M. M. Hurley and P. Harrowell, J. Chem. Phys. **105**, 10521 (1996).
- [11] D. N. Perera and P. Harrowell, J. Chem. Phys. **111**, 5441 (1999).
- [12] C. Reichhardt and C. J. O. Reichhardt, Phys. Rev. Lett. **90**, 095504 (2003).
- [13] A. H. Marcus, J. Schofield, and S. A. Rice, Phys. Rev. E **60**, 5727 (1999).
- [14] B. Cui, B. Lin, and S. A. Rice, J. Chem. Phys. **114**, 9142 (2001).
- [15] R. Zangi and S. A. Rice, Phys. Rev. E **58**, 7529 (1998).
- [16] S. A. Rice, Phys. Rev. **112**, 804 (1958).
- [17] S. A. Rice and N. H. Nachtrieb, J. Chem. Phys. **31**, 135 (1959).
- [18] R. Zwanzig, Phys. Rev. **156**, 190 (1967).
- [19] M. Buchner, B. M. Ladanyi, and R. M. Stratt, J. Chem. Phys. **97**, 8522 (1992).
- [20] T. Keyes, J. Chem. Phys. **101**, 5081 (1994).
- [21] V. Halpern, Philos. Mag. B **81**, 1237 (2001).